ChemComm

COMMUNICATION

View Article Online
View Journal | View Issue

Cite this: *Chem. Commun.*, 2025, **61**, 3696

Received 12th December 2024,
Accepted 3rd February 2025

DOI: 10.1039/d4cc06535b

rsc.li/chemcomm

Hypoelectronic titanaboranes: icosahedral and tetracapped tetrahedral clusters comprising bridging hydrides†

Subhash Bairagi, Debipada Chatterjee,‡ Soumen Giri‡ and Sundargopal Ghosh *

Unusual hypoelectronic *closo*-clusters, such as icosahedral $[(Cp^*Ti)_3(B_9H_7)(\mu_3\text{-}H)(\mu_3\text{-}Cl)_2]$ (1) and tetracapped tetrahedral $[\{(Cp^*Ti)_3B\}(\mu_3\text{-}BH_3)_2(\mu_3\text{-}Te)_2]$ (2), have been synthesized and structurally characterized. Clusters 1 and 2 represent the first examples of *closo*-titanaboranes having bridging hydrides, where the Ti···Ti interactions play a pivotal role in defining their shapes and electron counts. Furthermore, two face-fused clusters, $[(Cp^*Ti)_2(\mu\text{-}Se)(\mu\text{-}SePh)(\mu\text{-}\eta^3\text{:}\eta^3\text{-}B_5H_9R)]$ (3a: R = H; 3b: R = Ph), have been isolated that deviate from Mingos fusion formalism.

The electron-counting rules initially proposed by Wade and Williams[1,2] for single-cage boranes, and later extended by Mingos and Jemmis[3,4] for the single and fused polyhedral cages and their metal or main group derivatives, have been useful in understanding and classifying the structural and electronic properties of these compounds.[5–9] Based on geometries and skeletal electron pairs (SEPs), Wade and Williams classified the boron clusters as *closo* [$(n + 1)$ SEP], *nido* [$(n + 2)$ SEP], *arachno* [$(n + 3)$ SEP], and *hypho* [$(n + 4)$ SEP]. The relationship among these cluster geometries was further illustrated by a Rudolph diagram.[10] The successive removal of a vertex from a *closo* geometry, followed by the addition of bridging hydrogens (or 2e) to satisfy the electron count, generates *nido*, *arachno*, and *hypho*-geometries, respectively. Thus, *closo*-clusters, characterized by their high-symmetry spherical geometries, are inherently stable and typically do not require bridging hydrogens (or ligands) for stabilization.

Although *closo*-boron clusters are typically electronically saturated and obey the electron counting rules, a few hypoelectronic metallaboranes with such geometries have been reported.[5,9a,11–13] For instance, Kennedy and co-workers observed metallaboranes with *closo*-geometries that deviate from spherical deltahedra, possessing n SEPs instead of the expected $(n + 1)$ SEPs.[5b,11] These 'disobedient' metallaborane frameworks are often classified as *isocloso* or *hypercloso*-deltahedra, which can be derived from the corresponding *closo*-deltahedra by diamond-square-diamond (DSD) rearrangements. Fehlner and co-workers reported a series of hypoelectronic *closo*-rhenaboranes $[(Cp^*Re)_2B_nH_n]$ (n = 7–10, **I**, Chart 1), with $(n - 2)$ SEP that can be generated from canonical $[B_nH_n]^{2-}$ (n = 9–12) shapes by carrying out two or more DSD rearrangements.[12] Recently, we have isolated a series of hypoelectronic *closo*-osmaborane clusters $[(Cp^*Os)_2B_nH_n]$ (n = 6–10, **II**) with $(n - 1)$ SEP that show unusual less spherical deltahedral shapes.[13] These findings illustrate that the formal SEP can vary widely from the canonical number, and as it decreases, the cluster shape deviates from that of a more spherical deltahedron. On the other hand, hypoelectronic metallaboranes may also result when they comprise early transition metal fragments. These clusters are structurally diverse and exhibit high metal coordination numbers and cross-cluster bonding.[5b,9a,12]

Although various metallaboranes have been synthesized over the past six decades, relatively few examples of those containing early transition metals are known.[5,9,11–14] In this regard, group 4 metallaboranes are particularly scarce.[15–18] Barton and co-workers obtained a few group 4 metallaboranes by reacting anionic boranes with metal halides.[15] Using the same metal precursor, our group recently isolated zirconium and hafnium-guarded heptaborane and octaborane analogues.[16] Very recently, we synthesized and structurally characterized a supraicosahedral 16-vertex *hypho*-titanaborane (**III**)

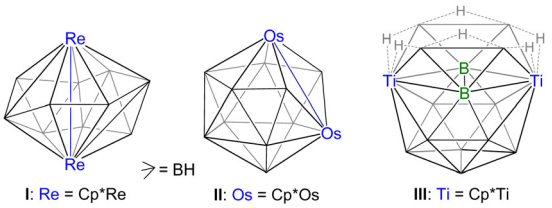

Chart 1 Examples of hypoelectronic *closo* (**I**, **II**) and *hypho* (**III**) metallaborane clusters.

Department of Chemistry, Indian Institute of Technology Madras, Chennai 600036, India. E-mail: sghosh@iitm.ac.in

† Electronic supplementary information (ESI) available. CCDC 2353840, 2321603, and 2385700. For ESI and crystallographic data in CIF or other electronic format see DOI: https://doi.org/10.1039/d4cc06535b

‡ These authors contributed equally to this work.

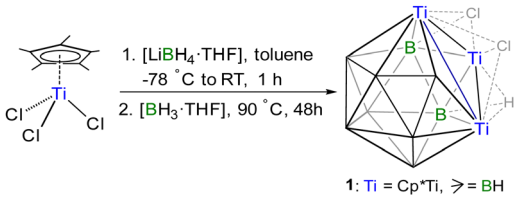

Scheme 1 Synthesis of icosahedral cluster **1**.

using monoborane pyrolysis methodology.[18] Encouraged by this achievement, we resumed our search for a *closo*-metallaborane cluster of titanium by varying the reaction conditions, which led to the isolation of the first two *closo*-titanaboranes with bridging hydrides.

The low-temperature reaction of [Cp*TiCl$_3$] with [LiBH$_4$] in toluene for 1 h, followed by thermolysis at 90 °C for 48 h in the presence of excess [BH$_3$·THF], afforded 12-vertex titanaborane cluster [(Cp*Ti)$_3$(B$_9$H$_7$)(μ$_3$-H)(μ$_3$-Cl)$_2$] (**1**) along with cluster **III** (Scheme 1 and Fig. S1, ESI†).[18] Compound **1** was isolated as a green solid in 12% yield. The ^{1}H NMR spectrum of **1** exhibited two distinct Cp* proton signals at δ = 2.03 and 2.05 ppm in 2 : 1 ratio, along with broad signals corresponding to terminal B–H protons in the downfield region and a broad resonance at δ = −5.67 ppm, attributed to μ$_3$-H bridging hydride. The ^{11}B{^{1}H} NMR spectrum displayed five broad resonances at δ = 31.6, 40.2, 45.0, 52.3, and 66.4 ppm in 4 : 2 : 1 : 1 : 1 ratio. The IR spectrum featured a band at 2544 cm^{-1}, characteristic of terminal B–H stretching vibrations. The mass spectrum displayed an isotopic distribution pattern at *m*/*z* 726.3257, corresponding to [M + H]$^+$. Furthermore, solid-state X-ray structure analysis was performed on a suitable crystal grown at 5 °C from a CH$_2$Cl$_2$–hexane solution.

The solid-state X-ray structure of **1** revealed a 12-vertex icosahedral geometry with one DSD rearrangement (Fig. 1). Interestingly, the presence of three Cp*Ti fragments in the icosahedral core significantly altered its geometry and SEP count. Although the connectivity pattern of **1** aligns with the *hypercloso* geometry, it possesses (*n* − 3) SEP and does not obey the Wade-Williams relationship.[1,2] Jemmis and co-workers have postulated that

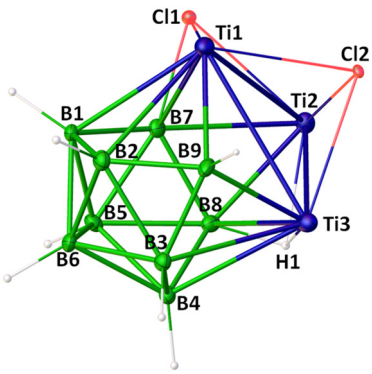

Fig. 1 Molecular structure and atom labelling diagram of **1**. Note that Cp* ligands attached to Ti atoms are omitted for clarity. Selected bond lengths (Å) and angles (°) in **1**: Ti–Ti3 3.073(3), Ti1–B1 2.513(16), Ti1–B9 2.174(15), B2–B9 1.61(2), B7–Cl1 1.854(19), Ti1–Cl1 2.543(5), B8–H1 1.19(3), Ti2–H1 1.95(13), Ti1–Ti2–Ti3 58.01(7), Ti1–B9–Ti3 91.3(6).

transition metals preferentially occupy the highest-degree vertices due to their more diffuse d-orbitals, which is consistent with the structural features of **1**.[19] In particular, two Ti atoms occupy two vertices of degree six and form a cross-cluster Ti–Ti bond, while the third Ti atom is occupied at a degree-four vertex. Most boron atoms occupy degree-five vertices, except for B9, which is at a degree-four vertex due to the DSD rearrangement. The B9–B2 (1.61(2) Å) and B9–B3 (1.61(2) Å) bond distances are shorter than other B–B bonds, likely reflecting the reduced connectivity of the B9 vertex. All boron atoms in **1** feature terminal hydrogens except for B7 and B8, which are bonded to bridging Cl and H ligands, respectively. These bridging ligands further interact with Ti1–Ti2 and Ti2–Ti3 centers in μ$_3$-fashion. The bulkier μ$_3$-Cl ligand around the Ti1–Ti2 region resulted in a longer Ti1–Ti2 bond length (3.292 Å) as compared to the other Ti–Ti bonds (3.026(3) Å and 3.073(3) Å). Additionally, a μ$_3$-Cl ligand bridges the Ti$_3$ face. Intriguingly, an intramolecular Cp*–H···Cl interaction is observed, with an H···Cl distance of 2.399 Å, shorter than the typical van der Waals separation. This suggests the possibility of weak hydrogen bonding between a Cp*–H and the Cl1 atom (Fig. S1, ESI†). The Ti–B bond lengths in **1** (av. 2.369 Å) are comparable to those observed in related titanaboranes such as **III**[18] (av. 2.409 Å), while the Ti–Ti bond distances (av. 3.130 Å) are significantly longer than those in [(Cp*Ti)$_2$(μ-η^6:η^6-B$_6$H$_6$)(μ-H)$_6$] (2.9307(12) Å).[17] The B–B bond lengths (av. 1.79 Å) are within the typical range for titanaborane clusters;[17,18] however, the anomalous B–B and Ti–B distances may be attributed to the presence of bridging ligands and one DSD rearrangement. Cluster **1** is the first example of a *closo*-icosahedron with bridging ligands.

The molecular structure of **1** also shows that the [Ti$_3$B$_9$] core is symmetrical with a symmetry plane containing Ti2, B5, B6, and B9 atoms. Its core geometry [Ti$_3$B$_9$] is comparable to that of recently reported metallaboranes [(Cp*M)$_2$B$_{10}$H$_{10}$] (M = RhH or IrH with *n* SEP; M = Os with (*n* − 1) SEP).[13] Similar to these clusters, the face in which the DSD rearrangement occurred is flattened in **1** (dihedral angle along B–Os–Os–B in **II** is 176.39°, along B–Ti–Ti–Ti in **1** is 173.30°). This flattening brings the Ti atoms closer, facilitating Ti–Ti bonding and forming an *oblato*-shape cluster. Among the *closo* 12-vertex clusters, **1** exhibits the lowest SEP count (*n* − 3), rendering it hypoelectronic and enabling the inclusion of bridging hydride and chloride ligands. While DSD-rearranged *closo*-metallaboranes such as M$_2$B$_{10}$ are known, **1** represents the first example of an M$_3$B$_9$ cluster with icosahedron geometry.

In metallaborane cluster chemistry, the choice of boron reagent plays a crucial role in isolating various metallaboranes with unique structural features. To explore this further, we modified the synthetic strategy by using [LiBH$_3$TePh] as the monoborane reagent instead of [LiBH$_4$]. As a result, the reaction of [Cp*TiCl$_3$] with three equivalents of [LiBH$_3$TePh] at −78 °C, followed by thermolysis at 80 °C for 18 h, yielded an 8-vertex *closo*-tetracapped tetrahedral cluster [{(Cp*Ti)$_3$B}(μ$_3$-BH$_3$)$_2$(μ$_3$-Te)$_2$] (**2**) as a yellow solid in 25% yield (Scheme 2). The ^{1}H NMR spectrum of **2** displayed two Cp* resonances at δ = 2.04 and 2.09 ppm in 1 : 2 ratio, along with signals corresponding to the terminal BH proton (δ = 2.36 ppm) and bridging Ti–H–B proton (δ = −2.79 ppm). The ^{11}B{^{1}H} NMR spectrum exhibited two resonances: a peak in the upfield region at δ = −7.7 ppm, assigned to the two-BH$_3$ boron,

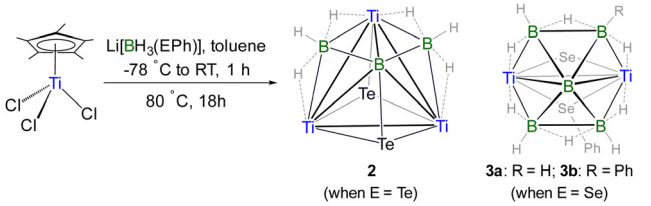

Scheme 2 Synthesis of tetracapped tetrahedral cluster **2** and face-fused clusters **3a–b** (Cp* ligands attached to Ti atoms in **2** and **3a–b** are omitted for clarity; Ti = Cp*Ti).

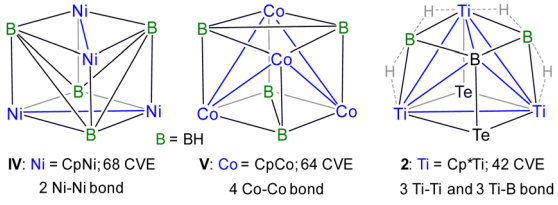

Chart 2 Experimentally known cubane-type geometry, along with its CVE count and the number of bonds present in the central tetrahedral unit.

and a downfield resonance at δ = 54.0 ppm, attributed to the boride boron, indicating a stronger boron–metal interaction. The molecular ion peak at *m*/*z* 845.1155 in ESI-MS was in good agreement with the molecular formula $[C_{30}H_{51}B_3Te_2Ti_3]$.

The solid-state X-ray structure of **2** revealed a $[Ti_3B]$ tetrahedral core with one boron and three titanium atoms occupying the corners of the tetrahedron, while two $\{BH_3\}$ fragments and two Te atoms capped its four faces (Fig. 2). For a tetrahedral $[M_3B]$ cluster, the SEP count is typically 6; however, **2** contains only 4 SEP.[1,2] The $[Ti_3B]$ core geometry of **2** is comparable to that of other triply bridging borylene complexes, such as $[(Cp^*Ru)_3(\mu\text{-}H)_3(\mu_3\text{-}BX)]$ (X = H, CN, OMe, OEt) with 4 SEP and $[\{(\eta^5\text{-}C_5H_4Me)Mn\}(CO)_2\{Pd(PCy_3)\}_2(\mu_3\text{-}BX)]$ (X = Cl, ^{t}Bu) with 3 SEP, where the borylene boron bears various substituents.[20] In **2**, three Ti atoms and one 'naked' B atom of the $[Ti_3B]$ tetrahedral core occupy the degree six vertices, while two B atoms and two Te atoms occupy the degree three vertices. The Ti–Ti (av. 3.077 (Å)) and Ti–B (av. 2.435 (Å)) bond lengths in **2** are consistent with single bond orders and are comparable to those observed in **1** and **III**.[18] All the internal angles in **2** deviated from a regular tetrahedron due to the shorter Ti–B bonds compared to Ti–Ti bonds along with the capping on each face by boron and heteroatoms.

Alternatively, the core geometry $[Ti_3B_3Te_2]$ of **2** can be described as a cubane consisting of three Ti, three B, and two Te atoms. While cubane-type sulfido clusters have been extensively studied, their selenido and tellurido counterparts have received relatively less attention, and cluster **2** represents a rare example of a cubane geometry incorporating tellurium atoms.[21] Although the qualitative shape of cubane clusters remains consistent, changes in M–M bond distances often reflect variations in the electronic structure due to the addition or removal of electrons.[5b] Earlier, Kennedy classified $[(CpNi)_4B_4H_4]$ and $[(CpCo)_4B_4H_4]$ as 68 and 64 cluster valence electrons (CVEs), respectively, featuring two and four metal–metal bonds (Chart 2).[5a,22] He also predicted that a hypothetical 60-electron $[(CpFe)_4B_4H_4]$ cluster would adopt a cubane structure with six Fe–Fe bonds, forming a fully bonded metal tetrahedron. The 60 CVE metallaborane $[(Cp^*Mo)_2(\mu_3\text{-}Se)_2B_2H(\mu\text{-}H)\{Fe(CO)_2\}_2Fe(CO)_3]$, which features a cubane geometry with six M–M bonds, serves as a bridge among these clusters.[23] In comparison, cluster **2** can be viewed as $[M_3E_5]$ (E = main group fragment), derived from $[M_4E_4]$ by replacing one of the metals with a boron atom. Therefore, cluster **2** should possess 50 CVEs with three M–M and three M–B bonds; however, the total number of CVEs available in **2** is 42. Unlike previously reported late transition metal cubane clusters,[21–23] this electron deficiency arises from the use of early transition metal titanium and the replacement of one metal vertex with a main group element, boron. The deficiency is partially compensated by the presence of four Ti–H–B bridging hydrogens. However, the inclusion of boron in the $[M_3B]$ tetrahedral core significantly distorts the cubane geometry, leading to a structure better described as a tetracapped tetrahedron rather than a true cubane.

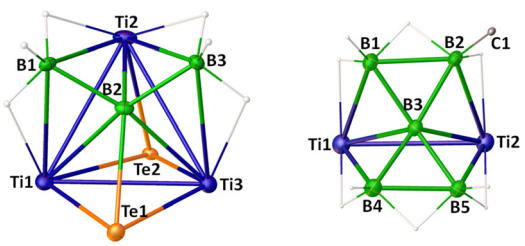

Fig. 2 Molecular structure and atom labelling diagram of **2** (left) and **3b** (right). Note that Cp* ligands attached to Ti atoms are omitted for clarity. Selected bond lengths (Å) and angles (°) in **2**: Ti1–Ti2 2.94683(13), Ti2–B2 2.279(9), Ti2–B3 2.547(15), Ti1–Ti2–Ti3 63.787, Ti1–B2–Ti2 80.358; **3b**: Ti1–Ti2 3.0281(7), Ti1–B3 2.271(4), Ti1–B3–Ti2 84.03(12).

After the effective isolation of the tetracapped tetrahedral cluster **2**, we have tried to isolate its selenium analogue by replacing $[LiBH_3TePh]$ with $[LiBH_3SePh]$ under similar reaction conditions. Although the targeted selenium analogue of **2** was not obtained, the reaction yielded two face-fused clusters, $[(Cp^*Ti)_2(\mu\text{-}Se)(\mu\text{-}SePh)(\mu\text{-}\eta^3\text{:}\eta^3\text{-}B_5H_9R)]$ (**3a**: R = H, 22%; **3b**: R = Ph, 17%, Scheme 2 and Scheme S3, ESI†). In **3a–b**, two *nido*-square pyramidal $[Ti_2B_3]$ geometries are fused through a common $[Ti_2B]$ triangle. Considering the Mingos fusion formalism, clusters **3a–b** require 62 electrons but possess 60 CVEs. Therefore, clusters **3a–b** can be classified as hypoelectronic clusters, which do not follow Mingos fusion formalism. Notably, similar to cluster **2**, these clusters feature a central "naked" boron atom, attributed to its high connectivity of degree six. Alternatively, **3a–b** can be described as a *hypho*-pentaborane cluster, where $[B_5H_9R]^{3-}$ is coordinated in a trihapto mode to each titanium center of the bimetallic template $[(Cp^*Ti)_2(\mu\text{-}SePh)(\mu\text{-}Se)]^{3+}$. Although **3a–b** resemble $[(Cp_2Zr)_2B_5H_8]^+$,[15] the presence of two bridging chalcogen ligands, which are intact with the titanium centers, allows the pentaborane ring to coordinate symmetrically to both metal centers (Fig. 2 and Fig. S5, S6, ESI†).

Density functional theory (DFT) studies show lower HOMO–LUMO gaps of 1.63 eV and 1.70 eV for **1** and **2**, respectively, that indirectly suggest their reduced kinetic and thermodynamic stability as compared to **III** (3.45 eV).[18] This reduced stability can be attributed to the change in the number of metal

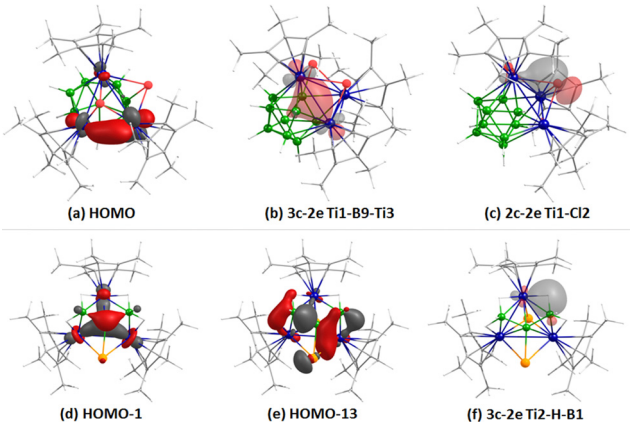

Fig. 3 Selected molecular orbitals (a), (d) and (e) and natural bond orbitals (b), (c) and (f) of clusters **1** (top) and **2** (bottom). Isocontour values: ±0.045 [e Bohr^{-3}]$^{1/2}$.

fragments, resulting in decreased SEP count relative to the parent clusters. Molecular orbital (MO) analysis of clusters **1** and **2** highlights strong Ti–Ti bonding interactions. For instance, the HOMO of **1** reveals significant bonding interactions between the d-orbitals of two Ti-atoms, indicating a Ti–Ti bond (Fig. 3a). In contrast, unlike cubane-type M_4E_4 geometries, the HOMO−1 of cluster **2** demonstrates triangular Ti_3 bonding interactions facilitated by the overlap of d-orbitals of the Ti-centers (Fig. 3d). Natural bond orbital (NBO) analysis further supports the Ti–Ti bonding in clusters **1** and **2**, with significant Wiberg bond indices (0.286, 0.421, and 0.535 for **1**; 0.382, 0.438 and 0.630 for **2**; Fig. 3b). Additionally, MO and NBO analyses of **1** and **2** reveal significant interactions between the Ti-centers and bridging ligands, which stabilize the clusters and influence their structural rearrangement, geometry, bonding orbitals, and electron count (Fig. 3c,e and f).

In summary, this work describes the isolation of *closo*-titanaboranes **1** and **2** featuring bridging hydrides. Theoretical studies and electron counting formalisms demonstrated that the presence of Ti–Ti bonds and bridging ligands play a crucial role in the stabilization of these hypoelectronic clusters. These findings emphasize the importance of early transition metal fragments in facilitating higher connectivity for the synthesis of novel non-Wadean structures in boron cages.

We gratefully acknowledge the generous support of SERB-DST (Scheme No. CRG/2023/000189), India, and the CoE on Molecular Materials and Functions under the IoE scheme, IIT Madras. S. B. and D. C. thank IIT Madras, and S. G. thanks UGC for fellowships. We also thank Dr B. Varghese, Dr P. K. S. Antharjanam, and Dr E. J. Packium for X-ray structure analysis.

Data availability

The data supporting this article have been included as part of the ESI.† Crystallographic data have been deposited at the CCDC under 2353840 (**1**), 2321603 (**2**), and 2385700 (**3b**).†

Conflicts of interest

There are no conflicts to declare.

Notes and references

1 (*a*) K. Wade, *J. Chem. Soc. D., Chem. Commun.*, 1971, 792; (*b*) K. Wade, *Inorg. Nucl. Chem. Lett.*, 1972, **8**, 559; (*c*) K. Wade, *Adv. Inorg. Chem. Radiochem.*, 1976, **18**, 1.
2 R. E. Williams, *Inorg. Chem.*, 1971, **10**, 210.
3 D. M. P. Mingos, *Acc. Chem. Res.*, 1984, **17**, 311.
4 E. D. Jemmis, M. M. Balakrishnarajan and P. D. Pancharatna, *J. Am. Chem. Soc.*, 2001, **123**, 4313.
5 (*a*) J. D. Kennedy, *Prog. Inorg. Chem.*, 1986, **34**, 211; (*b*) T. P. Fehlner, J.-F. Halet and J.-Y. Saillard, *Molecular Clusters A Bridge to Solid State Chemistry*, Cambridge University Press, Cambridge, United Kingdom, 2007.
6 (*a*) J. Zhang and Z. Xie, *Chem. – Asian J.*, 2010, **5**, 1742; (*b*) R. N. Grimes, *Carboranes*, Elsevier, Oxford, 2016.
7 (*a*) G.-X. Jin, *Coord. Chem. Rev.*, 2004, **248**, 587; (*b*) N. S. Hosmane, *Boron Science: New Technologies and Applications*, CRC, Boca Raton, FL, 2011.
8 (*a*) K. O. Kirlikovali, J. A. Axtell, A. Gonzalez, A. C. Phung, S. I. Khan and A. M. Spokoyny, *Chem. Sci.*, 2016, **7**, 5132; (*b*) J. Bould and J. D. Kennedy, *Chem. Commun.*, 2008, 2447.
9 (*a*) S. Kar, A. N. Pradhan and S. Ghosh, *Comprehensive Organometallic Chemistry IV*, ed. G. Parkin, K. Meyer and D. O'hare, Elsevier, Amsterdam, 2022, 9, pp. 263; (*b*) R. Borthakur, K. Saha, S. Kar and S. Ghosh, *Coord. Chem. Rev.*, 2019, **399**, 213021; (*c*) K. Saha, D. K. Roy, R. D. Dewhurst, S. Ghosh and H. Braunschweig, *Acc. Chem. Res.*, 2021, **54**, 1260.
10 (*a*) R. W. Rudolph, *Acc. Chem. Res.*, 1976, **9**, 446; (*b*) S. Kar, S. Bairagi, G. Joshi, E. D. Jemmis, H. Himmel and S. Ghosh, *Acc. Chem. Res.*, 2024, **57**, 2901.
11 (*a*) J. D. Kennedy, Disobedient Skeletons, in *The Borane, Carborane, Carbocation Continuum*, ed. J. Casanova, Wiley, New York, 1998, p. 85; (*b*) J. D. Kennedy, *Prog. Inorg. Chem.*, 1984, **32**, 519; (*c*) R. L. Johnston, D. M. P. Mingos and P. Sherwood, *New J. Chem.*, 1991, **15**, 831.
12 (*a*) B. L. Guennic, H. Jiao, S. Kahlal, J.-Y. Saillard, J.-F. Halet, S. Ghosh, M. Shang, A. M. Beatty, A. L. Rheingold and T. P. Fehlner, *J. Am. Chem. Soc.*, 2004, **126**, 3203; (*b*) S. Ghosh, B. C. Noll and T. P. Fehlner, *Angew. Chem., int. Ed.*, 2005, **44**, 2916.
13 (*a*) K. Kar, S. Kar and S. Ghosh, *Chem. Sci.*, 2024, **15**, 4179; (*b*) D. K. Roy, B. Mondal, P. Shankhari, R. S. Anju, K. Geetharani, M. Mobin and S. Ghosh, *Inorg. Chem.*, 2013, **52**, 6705.
14 (*a*) S. Aldridge, M. Shang and T. P. Fehlner, *J. Am. Chem. Soc.*, 1998, **120**, 2586; (*b*) A. S. Weller and T. P. Fehlner, *Organometallics*, 1999, **18**, 447; (*c*) R. S. Anju, D. K. Roy, K. Geetharani, B. Mondal, B. Varghese and S. Ghosh, *Dalton Trans.*, 2013, **42**, 12828.
15 R. L. Thomas, N. P. Rath and L. Barton, *J. Am. Chem. Soc.*, 1997, **119**, 12358.
16 (*a*) A. De, Q. Zhang, B. Mondal, L. F. Cheung, S. Kar, K. Saha, L. Wang and S. Ghosh, *Chem. Sci.*, 2018, **9**, 1976; (*b*) S. Kar, S. Bairagi, G. Joshi, E. D. Jemmis and S. Ghosh, *Chem. – Eur. J.*, 2021, **27**, 15634.
17 S. Kar, S. Bairagi, A. Haridas, G. Joshi, E. D. Jemmis and S. Ghosh, *Angew. Chem., Int. Ed.*, 2022, **61**, e202208293.
18 S. Kar, S. Bairagi, J.-F. Halet and S. Ghosh, *Chem. Commun.*, 2023, **59**, 11676.
19 E. D. Jemmis, *J. Am. Chem. Soc.*, 1982, **104**, 7017.
20 (*a*) R. Okamura, K. Tada, K. Matsubara, M. Oshima and H. Suzuki, *Organometallics*, 2011, **20**, 4772; (*b*) H. Braunschweig, C. Burschka, M. Burzler, S. Metz and K. Radacki, *Angew. Chem., Int. Ed.*, 2006, **45**, 4352; (*c*) K. Yuvaraj, D. K. Roy, K. Geetharani, B. Mondal, V. P. Anju, P. Shankhari, V. Ramkumar and S. Ghosh, *Organometallics*, 2013, **32**, 2705.
21 (*a*) E. I. Stiefel and K. Matsumoto, *Transition Metal Sulfur Chemistry*, Honolulu, Hawaii, 1995; (*b*) R. Llusar, S. Uriel and C. Vicent, *J. Chem. Soc., Dalton Trans.*, 2001, 2813; (*c*) A. Thakur, S. Sao, V. Ramkumar and S. Ghosh, *Inorg. Chem.*, 2012, **51**, 8322.
22 (*a*) J. R. Bowser, A. Bonny, J. R. Pipal and R. N. Grimes, *J. Am. Chem. Soc.*, 1979, **101**, 6229; (*b*) J. R. Pipal and R. N. Grimes, *Inorg. Chem.*, 1979, **18**, 257.
23 K. Geetharani, S. K. Bose, S. Sahoo and S. Ghosh, *Angew. Chem., Int. Ed.*, 2011, **50**, 3908.